Ultrasonics Sonochemistry 95 (2023) 106383

Contents lists available at ScienceDirect

Ultrasonics Sonochemistry

journal homepage: www.elsevier.com/locate/ultson

Ultrasonic assisted extraction, characterization and gut microbiota-dependent anti-obesity effect of polysaccharide from Pericarpium Citri Reticulatae 'Chachiensis'

Yapeng Li [a,b,1], Zi Li [a,b,1], Baizhong Chen [c], Yajun Hou [a,b], Yilin Wen [a], Lishe Gan [a,b], Jinwei Jin [a,b], Chen Li [a,b], Panpan Wu [a,b], Dongli Li [a,b,*], Wen-Hua Chen [a,*], Rihui Wu [a,b,*]

[a] School of Biotechnology and Health Sciences, Wuyi University, Jiangmen 529020, PR China
[b] International Healthcare Innovation Institute (Jiangmen), Jiangmen 529040, PR China
[c] Guangdong Xinbaotang Biotechnology Co. Ltd., Jiangmen 529100, PR China

ARTICLE INFO

Keywords:
Pericarpium Citri Reticulatae 'Chachiensis'
Polysaccharide
Gut microbiota
Ultrasound-assisted extraction
Obesity

ABSTRACT

Pericarpium Citri Reticulatae 'Chachiensis' (PCRC), the premium aged pericarps of Pericarpium Citri Reticulatae, is widely used in traditional Chinese medicines with a diversity of promising bioactivity. Herein we report the extraction, characterization and underlying mechanism of anti-metabolic syndrome of an arabinan-rich polysaccharide from PCRC (PCRCP). This polysaccharide was obtained in a 7.0% yield by using ultrasound-assisted extraction under the optimized conditions of 30 mL/g liquid-to-solid ratio, 250 W ultrasound power for 20 min at 90 °C with pH 4.5. The PCRCP with an average molecular weight of 122.0 kDa, is mainly composed of D-galacturonic acid, arabinose and galactose, which may link *via* 1,4-linked Gal(p)-UA, 1,4-linked Ara(f) and 1,4-linked Gal(p). Supplementation with PCRCP not only effectively alleviated the weight gain, adiposity and hyperglycemia, but also regulated the key metabolic pathways involved in the *de novo* synthesis and β-oxidation of fatty acid in high-fat diet (HFD)-fed mice. Furthermore, PCRCP treatment caused a significant normalization in the intestinal barrier and composition of gut microbiota in mice fed by HFD. Notably, PCRCP selectively enriched *Lactobacillus johnsonii* at the family-genus-species levels, a known commensal bacterium, the level of which was decreased in mice fed by HFD. The depletion of microbiome induced by antibiotics, significantly compromised the effects of anti-metabolic syndrome of PCRCP in mice fed by HFD, demonstrating that the protective phenotype of PCRCP against anti-obesity is dependent on gut microbiota. PCRCP is exploitable as a potential prebiotic for the intervention of obesity and its complications.

1. Introduction

Pericarpium Citri Reticulatae (PCR) is the dried and aged pericarp of *Citrus reticulata* Blanco (Rutaceae) and its cultivars, and also known as Chenpi in Chinese. It has been generally used as herbal medicines for treating the spleen deficiency-related, indigestive, respiratory and inflammatory diseases, including COVID-19 [3]. Because of its unique aroma, preeminent pharmacological effect and low toxicity, PCR is frequently consumed as food, dietary seasoning and tea ingredients. Notably, among the main Chenpi cultivars, Pericarpium Citri Reticulatae 'Chachiensis' (PCRC, also called as Guangchenpi in Chinese) is recognized as the most premium PCR in both Chinese and American Pharmacopoeia [39]. Phytochemical investigations have indicated that PCR is abundant in active ingredients, including essential oils, polyphenols, flavonoids and polysaccharides, thus offering a diversity of biofunctionality including strong antioxidant, anti-inflammatory and immunoregulatory activity [14,31]. For example, previous studies have reported the effects of anti-liver injury and anti-obesity of flavonoids from PCR [35,40]. Among these bioactive ingredients in PCR, polysaccharides act as one of the most important components and display an excellent intestinal immune-modulating activity [27]. On the other hand, it is well recognized that the quality, composition and bioactivity of polysaccharides are closely related to the source and extraction methods. However, the extraction, physicochemical characteristics and

* Corresponding authors at: School of Biotechnology and Health Sciences, Wuyi University, Jiangmen 529020, PR China.
E-mail addresses: wyuchemldl@126.com (D. Li), whchen@wyu.edu.cn (W.-H. Chen), wyuchemwrh@126.com (R. Wu).
[1] These authors contributed equally to this work.

https://doi.org/10.1016/j.ultsonch.2023.106383
Received 21 December 2022; Received in revised form 20 February 2023; Accepted 23 March 2023
Available online 27 March 2023

bioactivity of polysaccharides from PCRC (PCRCPs) have been rarely explored to date.

Due to the unique chemical structures and diverse biological activity, bioactive polysaccharides from traditional Chinese medicines have attracted extensive attention. However, polysaccharides, for example the ones from Chinese herbal medicines (CHPs) cannot be broken down by human endogenous enzymes and absorbed in stomach. Ingested CHPs can be utilized by the intestinal microorganisms that resident in the large intestine. These gut microorganisms encode a large number of enzymes that can degrade CHPs into oligosaccharides and monosaccharides [34]. The degraded oligosaccharides and monosaccharides, can not only selectively boost the growth of gut beneficial bacteria and reshape the structure and composition of microorganisms, but also can be digested into short-chain fatty acids (SCFAs). These bacterial species and SCFAs may interact closely with intestinal cells, and exert their beneficial effects [21].

Recently, gut microbiome has emerged as an important regulator for energy acquisition, storage and anabolism [7]. Abnormal composition or function of gut microorganisms might result in a disturbance of energy and substrate metabolism in adipose tissue, muscle and liver [12]. In fact, a number of traits, such as adiposity, insulin resistance and dyslipidaemia have been observed in individuals with metabolic disorders. Therefore, strategies that are able to modulate gut microbiome have been proposed to prevent and alleviate metabolic disorders [1]. Several animal and human studies have shown that consumption of polysaccharides and dietary fibre can potently regulate specific anti-obesogenic microorganisms and their metabolites, and exert the improvements of intestinal integrity, obesity and metabolic symptoms [29,36]. Apart from the changed gut microbiota and microbial-derived fermentation, polysaccharides and their derivatives can mitigate metabolic syndrome (MetS) by regulating different cellular signal pathways, such as peroxisome proliferator-activated receptors, 5′-adenosine monophosphate-activated protein kinases, and CCAAT/enhancer binding protein-α (Wang et al., 2018). These findings make us reasoning that PCRCPs might serve as potential prebiotics to enrich health-promoting bacteria, regulate molecular signaling pathway and ameliorate MetS.

In the work described herein, we sought to readily access PCRCPs and explore their gut microbiota-dependent anti-obesity effects. Specifically, we extracted soluble PCRCPs by using ultrasound-assisted extraction (UAE), optimized its conditions based on response surface methodology (RSM), and analyzed its structure, including the monosaccharide compositions, molecular weight and glycosidic linkages by using chemical and spectroscopic methods. Importantly, we systematically investigated the effects of PCRCP on the obesity, hypoglycemic and lipid dyshomeostasis in mice fed with a high-fat diet (HFD), and used 16S rDNA-based microbiota analysis and RNA-sequence profiling to clarify the shifted bacterial species and molecular signaling pathways. In addition, we carried out antibiotic treatment experiments to further uncover the potential mechanisms that involved in the anti-obesity of gut microbiota revised by PCRCP. Herein we report our findings in details.

2. Materials and methods

2.1. Raw materials and chemicals

PCRC samples were collected in 2018 and obtained as a gift from Guangdong Xinbaotang Biotechnology Co. Ltd. (Jiangmen, Guangdong, China). They were pulverized into powder and sieved by an 80-mesh screen. All the other chemical reagents were purchased locally and are analytical grade.

2.2. Preparation and physicochemical characterizations of PCRCP

2.2.1. Design of single-factor experiments

The UAE of PCRCP was performed with a previous protocol with slight modification (Gu et al., 2020). In brief, 100 g PCRC powder was extracted with 95% (v/v) ethanol in a reflux device at 80 °C for 3 h to remove colored substances, amino acids, monosaccharides and other compounds with low molecular weights. The obtained residue was oven-dried at 60 °C to constant weight. An ultrasonic apparatus was used to perform the UAE of PCRCP, under the condition of different liquid to solid ratios (A: 10, 15, 20, 25, 30 and 35 mL/g), pH (B: 4, 4.5, 5, 5.5, 6 and 6.5), temperature (C: 70, 75, 80, 85, 90 and 95 °C), ultrasonic power (D: 50, 100, 150, 200, 250 and 300 W), ultrasonic time (E: 5, 10, 15, 20, 25 and 30 min), and extract time (20 min). The extracted solution was diluted with four volumes of ethanol (95% v/v), then stewing overnight at 4 °C. The formed precipitate was washed subsequently with alcohol, ether and acetone, and re-dissolved in distilled water. The resulting aqueous solution was decolorized with polyamides, deproteinized with a Sevag method, and finally freeze-dried to afford crude PCRCP. The extraction yield (Y%) was determined as the weight of dried PCRCP (W_{PCRCP}) relative to the weight of pre-treated PCRC powder (W), that is, $Y\% = W_{PCRCP}/W \times 100\%$.

2.2.2. Box-Benhnken design

A five-factor three-level Box-Behnken design (BBD) was used to optimize the UAE process. The BBD was designed using a Design-Expert software (Version 10.0.5, Stat-Ease Inc., USA) and represented in Table S1. The extraction yield of PCRCP (Y%) was selected as the response (three replicates). The adequacy of the regression model was determined by the coefficients adjusted-R^2 and R^2, and the significant difference between the regression model and the coefficient was assessed by an F test.

2.2.3. Purification of crude polysaccharides

The extracted polysaccharides were purified by using a reported three-phase method. Briefly, 5 g of crude polysaccharide, 200 g of ammonium sulfate and 50 mL of *t*-butanol were added to 500 mL of water. The solution was mixed fully and then allowed to stand at 4 °C for 24 h. Finally, the formed mixture was centrifuged (3000 rpm, 15 min), dialyzed and freeze-dried to give PCRCP.

2.2.4. Determination of chemical composition

The total carbohydrates, proteins, uronic acid and polyphenols in PCRCP were determined by using a phenol-H_2SO_4 method, a Bradford method, an *m*-hydroxybiphenyl method, and a folin-phenol reagent, respectively [13].

2.2.5. Composition, IR spectral analysis and molecular weight of PCRCP

For the determination of the compositions of PCRCP, a solution of PCRCP (5 mg) in aqueous CF_3COOH (2 M, 1 mL) was heated at 120 °C for 2 h. After concentrating the solution with nitrogen, the precipitate was dissolved in methanol and dried with nitrogen. The obtained residue was re-dissolved in deionized water and filtered through a 0.45 μm membrane. The filtrate was analyzed using a high-performance anion-exchange chromatography (HPAEC, Thermo Fisher Scientific, USA) equipped with a CarboPac PA-20 anion-exchange column (3 × 150 mm; Dionex) and a pulsed amperometric detector (Dionex ICS 5000 system, Thermo Fisher Scientific, USA).

The IR spectra of PCRCP were measured on a Fourier transform-infrared spectrophotometer (FT-IR) (Bruker, Karlsruhe, Germany) using a KBr tablet method.

For the measurement of average molecular weight (MW), the sample was dissolved in a 0.1 M $NaNO_3$ solution and filtered through a 0.45 μm membrane. The filtrate was injected into a high performance gel permeation chromatography (HPGPC) (Waters Division Millipore, Milford, MA, USA) combined with a refractive index detector and two serially connected ultra-hydrogel linear columns. The column was eluted with deionized water at a flow rate of 0.8 mL/min. The MW was determined by calibration curve based on the standards of several dextrans. An empower software (Waters Corp., Milford, MA, USA) was used

for data processing and analysis.

2.2.6. Analysis of glycosidic linkages

PCRCP was methylated using NaOH-DMSO-MeI according to a previously reported procedure [23]. In brief, the mixture of PCRCP (5 mg), DMSO (2 mL) and NaOH (30 mg) was stirred for 3 h. To the mixture was added 50 μL MeI and the reaction was conducted for further 1 h, followed by the addition of a mixture of 1 mL H_2O and 2 mL CH_2Cl_2. The methylated products were subjected to methanolysis with 3.5% MeOH-HCl (1 mL) at 80 °C for 2 h, followed by hydrolysis with H_2SO_4 (1 M, 1 mL) at 100 °C for 27 h. The solution was neutralized with $BaCO_3$ and reduced with $NaBH_4$ and acetylated. The prepared methylated alditol acetates were filtered by a 0.22 μm membrane and analyzed by gas chromatography-mass spectrometry (GC–MS) (Agilent Technologies, USA) on a column SH-RTX-5 ms.

2.3. Anti-obesity activity of PCRCP in mice

2.3.1. Experimental design and drug administration

The animal experiments were ethically approved by the Committee on the Ethics of Animal Experiments of International Healthcare Innovation Institute (Jiangmen, China). All animal-related experimental protocols were conducted consistently with the Guidelines for the Care and Use of Laboratory Animals of this institution. Briefly, male C57BL/6J mice (eight-week-old, body weight 20 ± 2 g) were purchased from Guangdong Medical Animal Center (Foshan, China). Mice were housed at a constant temperature and humidity with 12 h/12 h light/dark cycle for one week. Mice were fed with either a standard chow diet (Chow, 10% fat, 3.5 kcal/g diet) or high-fat diet (HFD, 45% fat, 16.8 kcal/g diet, Table S2) with or without a oral dosage of 60 mg/kg/d PCRCP for four weeks (n = 5–7). For the antibiotic treatment, a mixture of ABX, vancomycin (0.5 g/L) and neomycin sulfate (1 g/L) was supplemented in daily dinking water.

Body weight and food intake were taken weekly. After four weeks of treatment, fresh fecal were collected and frozen with liquid nitrogen, stored for microbial sequencing analysis. Plasma was collected, and the liver, and gonadal, inguinal and perirenal white adipose tissues (gWAT, iWAT and pWAT) were precisely dissected and weighed.

2.3.2. Fasting blood glucose and oral glucose tolerance test (OGTT)

The OGTT were carried out after the treatment of PCRCP. In brief, the overnight-fasted mice were administrated orally with 2.0 g/kg single-dose D-glucose, the levels of blood glucose were monitored with an Accu-Chek glucose monitor (Roche Diagnostics GmbH, Germany) at 0, 15, 30, 60, 90 and 120 min, respectively.

2.3.3. Biochemical analysis

Plasma levels of total cholesterol (CHO), total triacylglycerol (TG), low-density lipoprotein-cholesterol (LDL-C), alanine aminotransferase (ALT) and aspartate aminotransferase (AST) were quantified on an automatic analyzer (FAITH-1000, Nanjing Laura Electronics Co., Ltd., Nanjing, China) based on commercial ELISA kits (BioSino Bio-Technology and Science Inc., Beijing, China).

2.3.4. Haematoxylin and eosin (H&E) staining

The gWAT, liver and small intestine tissues were paraform-fixed, dehydrated and embedded in paraffin. 3 μm paraffin-embedded sections were cut with a Leica RM22559 microtome (Leica, Wetzlar, Germany) and stained with H&E under the standard procedures. Pictures were photographed on an Olympus BX41 microscope (Olympus Corporation, Tokyo, Japan).

2.3.5. RNA sequencing (RNA_seq) analysis

Total RNA was extracted from gWAT by using a TRIZOL reagent (Invitrogen, USA) and quantified with an Agilent Bioanalyzer 2100 system (Agilent Technologies, San Diego, CA, USA). The establishment of cDNA library was performed by using mRNA_Seq preparation kit (Illumina, San Diego, USA) according to the manufacturer's instructions. The constructed sequencing libraries were sequenced with the paired-end technology on an Illumina sequencing platform (Illumina HiSeq 4000) at the Beijing Biomarker Technologies Co. (Beijing, China). The low quality reads were filtered with a R bioconductor project DEbrowser. The clean data were submitted and aligned to the mouse reference genome (https://www.ncbi.nlm.nih.gov/bioproject/PRJNA169). The differential expressed genes were identified using DESeq2 package with a threshold of $P_{adj} < 0.01$ and $|\log2 \text{ Fold Change}|$ greater than1.5. Clusters of Orthologous Groups (COG) enrichment and KEGG pathway enrichment were analyzed and visualized using a BMKCloud platform (https://www.biocloud.net). Gene expression level (FPKM) was quantified by a RNA-Seq by Expectation Maximization (RSEM) software package.

2.3.6. 16S rDNA amplicon sequencing

The genomic DNA was extracted from stool bacteria by using a commercial kit (TIANGEN Biotech Co. Ltd., Beijing, China) and quantified with an Agilent Bioanalyzer 2100 system (Agilent Technologies, San Diego, CA, USA). 16S rDNA genes of V3-V4 regions were amplificated using a MetaVx Library Preparation kit with specific primers. The purification of the DNA products was conducted with a Qiagen Gel Extraction Kit. DNA library quality was validated and sequenced on a PacBio platform at Biomarker Technologies Co, Ltd. (Beijing, China). The raw data were analyzed with Quantitative Insights into Microbial Ecology (QIIME) software package in BMK Cloud (https://www.biocloud.net). The bacteria with differential abundance were identified by the LEfSe analysis.

2.4. Data availability

The RNA sequencing data of adipose tissue and fecal microbiota have been submitted to the NCBI Sequence Read Archive (SRA) database (Accession number PRJNA895224 and PRJNA895530).

2.5. Statistics

Unless otherwise specified, data present the mean ± s.e.m. Statistical tests were performed by using a GraphPad Prism 9.0. Differences between groups were tested by a Student's t-test or one-way ANOVA followed by multiple comparisons. A value of $P < 0.05$ was recognized as statistically significant.

3. Results and discussion

3.1. Extraction and optimization of PCRCP by UAE

As the extraction yield and bioactivity of natural polysaccharides are affected by extraction methods and conditions [6], and UAE has been regarded as one of the most promising techniques with the advantages of high efficiency, low consumption of energy and solvents, and high yields (Gu et al., 2020), we studied and optimized the effect of UAE conditions on PCRCP extraction. The results of single-factor experiments are presented in Fig. 1. With the increase in the liquid-to-solid ratios, pH, temperature, ultrasonic power and ultrasonic time, the yield of PCRCP gradually increased and then decreased after reaching the maximum value, suggesting that these factors have remarkable effects on the extraction yield of PCRCP. The maximum yield may be obtained under the condition of the liquid-to-material ratios (25–35 mL/g), pH (4–5), temperature (85–95 °C), ultrasonic power (200–300 W) and ultrasonic time (15–25 min). Thus, these parameters were selected for further experiments based on response surface methodology (RSM). The results for the response value of BBD experiments and the analysis of variance of regression model were displayed in Table S3 and Table 1, respectively. The optimized extraction parameters of PCRCP were determined as

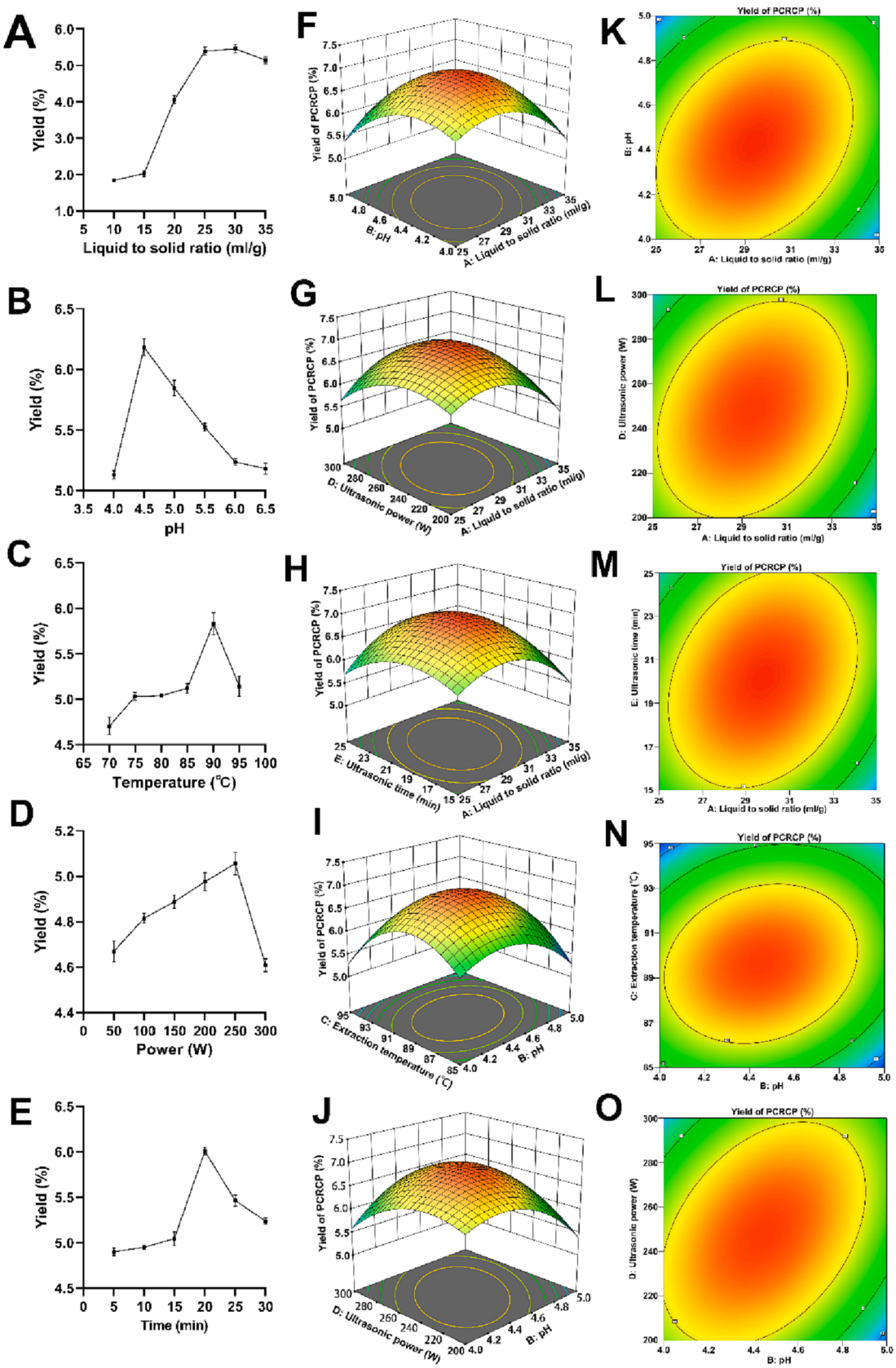

Fig. 1. Effects of ultrasound-assisted processes on the extraction yield of PCRCP and the plots of response surfaces analyses (three replicates). (A-E) Effects of liquid-to-solid ratios, pH, temperature, ultrasonic power and ultrasonic time on the yields of PCRCP. (F-J) Response surface diagram and (K-O) contour plots of the interaction of different variables on the yields of PCRCP.

Table 1
Analysis of variance for a fitted regression equation of the PCRCP yields.

Variables	Sum of squares	DF	Mean square	*F* value	*p*-value
Model	10.99	20	0.55	25.39	<0.0001
A	0.042	1	0.042	1.94	0.1758
B	0.22	1	0.22	10.10	0.0039
C	0.073	1	0.073	3.37	0.0784
D	0.047	1	0.047	2.19	0.1518
E	0.027	1	0.027	1.26	0.2727
AB	0.47	1	0.47	21.68	<0.0001
AC	0.20	1	0.20	9.36	0.0052
AD	0.36	1	0.36	16.63	0.0004
AE	0.30	1	0.30	13.72	0.0011
BC	0.22	1	0.22	10.21	0.0038
BD	0.61	1	0.61	28.11	<0.0001
BE	0.048	1	0.048	2.24	0.1474
CD	0.081	1	0.081	3.75	0.0641
CE	0.076	1	0.076	3.49	0.0734
DE	0.18	1	0.18	8.15	0.0085
A^2	3.16	1	3.16	146.15	<0.0001
B^2	2.72	1	2.72	125.5	<0.0001
C^2	5.85	1	5.85	270.27	<0.0001
D^2	1.87	1	1.87	86.40	<0.0001
E^2	1.77	1	1.77	91.79	<0.0001
Residual	0.54	25	0.022		
Lack of fit	0.51	20	0.026	4.52	0.0508
Pure error	0.028	5	0.0057		
Cor total	11.53	45			

$R^2 = 0.9531$; $R^2_{adj} = 0.9155$; $R^2_{pred} = 0.8186$; Adeq precision = 16.720; Coefficient of the variation C.V.% = 2.49.

follows: liquid-to-material ratio of 29.30 mL/g, pH of 4.40, extraction temperature of 89.51 °C, ultrasonic power of 245.63 W and ultrasonic time of 19.96 min. Under these conditions, the maximum predicted extraction yield of PCRCP was 6.94 ± 0.09%. To facilitate actual operation, these optimal parameters were set as liquid-to-material ratio, 30.0 mL/g; pH, 4.4; temperature, 90.0 °C; ultrasonic power, 250.0 W and ultrasonic time, 20.0 min. These optimal predicted conditions were further re-examined by three additional experiments. The actual average yield of PCRCP was 7.0 ± 0.02%, very similar to the predicted value of 6.94 ± 0.09%. More importantly, this yield of PCRCP was significantly higher than previous extraction yield (2.2%) of polysaccharides from 5-year PCRC using a conventional water extraction method [27]. These findings point out that the RSM model was reasonably used for the optimization of UAE, and these optimization conditions could effectively improve the extraction efficiency of polysaccharides from PCRC.

3.2. Chemical characterizations of PCRCP

The determination results of chemical compositions in PCRCP were shown in Table 2. The contents of carbohydrate and uronic acid were 66.0% and 28.0%, respectively, indicating that PCRCP is an acidic polysaccharide. HPGPC analysis shows that PCRCP has an average molecular weight of 122.0 kDa based on the dextran standard (Fig. S1A), which is consistent with the molecular weight range of polysaccharides from tangerine peels, 17.8–373 kDa [27,19]. By using the HPAEC, the main monosaccharides in PCRCP were detected as D-galacturonic acid (51.17%), arabinose (25.63%), galactose (12.25%) and glucose (5.46%) (Table 2 and Fig. S1B). The FT-IR spectrum of PCRCP reveals the presence of hydroxy (3447 cm^{-1}), methyl (2853 cm^{-1}), methylene (2924 cm^{-1}), acetyl C = O (1760–1740 cm^{-1}), C-O (1650–1578 cm^{-1}) and C-O-C (1091–1030 cm^{-1}) groups (Fig. S1C). Moreover, the probable glycosidic linkages of PCRCP were detected and shown in Table S4. The molar ratio of 1,4-linked Gal(p)-UA, 1,4-linked Gal(p) and 1,4-linked Ara(f) in PCRCP was determined to be 55.2: 9.7: 8.5, indicative of (1 → 4)- galacturonic acid, arabinose and galactose residues as the major backbones. These results suggest that PCRCP is an arabinan-rich pectic polysaccharide with a complex structure.

Table 2
Chemical compositions and monosaccharides of PCRCP.

Composition	w/w %	Monosaccharide	mol %
Carbohydrate	66.0	Galacturonic acid (Gal-UA)	51.17
Uronic acid	28.0	Arabinose (Ara)	25.63
Water	4.8	Galactose (Gal)	12.25
Protein	0.59	Glucose (Glc)	5.46
Polyphenol	0.25	Xylose (Xyl)	2.48

3.3. Gut microbiota-dependent anti-obesity of PCRCP in vivo

3.3.1. PCRCP ameliorates HFD-induced obesity and hyperlipidemia in mice

It is reported that D-galacturonic acid and arabinan present in a polysaccharide may be primarily responsible for its biological functions, such as for the treatment of various gastrointestinal symptoms, hyperglycaemia and hyperlipemia [8]. These findings inspired us to infer that PCRCP may be able to ameliorate HFD-induced obesity. To verify this, HFD-fed mice were administrated orally with PCRCP for four weeks (Fig. 2A). Compared with chow feeding mice, HFD feeding caused a conspicuous increase in daily energy intake and the weights of body, gWAT, iWAT and pWAT in mice (Fig. 2B-F). These observations are in line with previous studies [2,9,25], and clearly suggest that 4-week HFD feeding is sufficient enough to induce an animal model of obesity. In contrast, treatment with PCRCP markedly abated body weight and excess adipose tissue accumulation (Fig. 2B-F), but without any effect on daily energy intake and liver weight in mice fed with HFD (Fig. 2G and H), suggesting that the inhibitory effect of PCRCP on HFD-induced obesity was independent of appetite.

Hyperglycaemia and lipid dysmetabolism are usually induced by HFD, and thus are serious risk factors for metabolism-related diseases [10]. Therefore, we also determined the blood glucose, lipids and liver function enzymes. Compared with control mice, a notable increase in the level of fasting blood glucose and impaired glucose tolerance was found in HFD-fed mice. These phenotypes were profoundly ameliorated after treatment with PCRCP (Fig. 2I-K). Furthermore, PCRCP treatment normalized the levels of plasma TG, CHO, LDL-C, ALT and AST in mice fed by HFD (Fig. 2L-P). Consistent with the improvement of hyperglycaemia and lipid metabolism, PCRCP not only reduced adipocyte size and the number of the necrotic adipocytes and macrophages forming crown-like structures, but also decreased liver cell hypertrophy and steatosis in the liver lobules (Fig. 2Q). These findings indicate that PCRCP produced excellent anti-obesogenic and anti-diabetic effects in a HFD fed mouse model.

3.3.2. PCRCP regulates adipose gene expression profiles in mice fed with HFD

To reveal the underlying mechanism of PCRCP that is in charge of preventing obesity caused by HFD, we conducted an unbiased RNA sequencing (RNA_seq) to analyze the transcriptomic profiles of gWAT. Each sample generated 37,894,530 to 52,800,496 sequence reads (Table S5). The principal component analysis (PCA) showed that PCRCP treatment resulted in a distinct separation in gene expression (Fig. 3A). Next, we analyzed the genes differently expressed (DEGs) and Clusters of Orthologous Groups term (COG) functional classifications using DESeq2_edgeR tools ($P \leq 0.01$, fold change ≥ 1.5) on the platform BMKCloud (https://www.biocloud.net). In agreement with our above observation on the anti-MetS effect of PCRCP, the transcriptomic analysis showed 513 DEGs, including 258 downregulated and 255 upregulated genes (Fig. 3B) in PCRCP-fed mice, when compared to that of HFD-fed mice. The GO functional classification and KEGG pathway enrichment analysis presented that these DEGs were mainly enriched in complement and coagulation cascades, protein digestion and absorption, cholesterol metabolism, PPAR signaling pathway, and insulin resistance (Fig. 3C). Moreover, COG functional classifications of all DEGs revealed that PCRCP treatment regulated genes involved in the regulation of lipid,

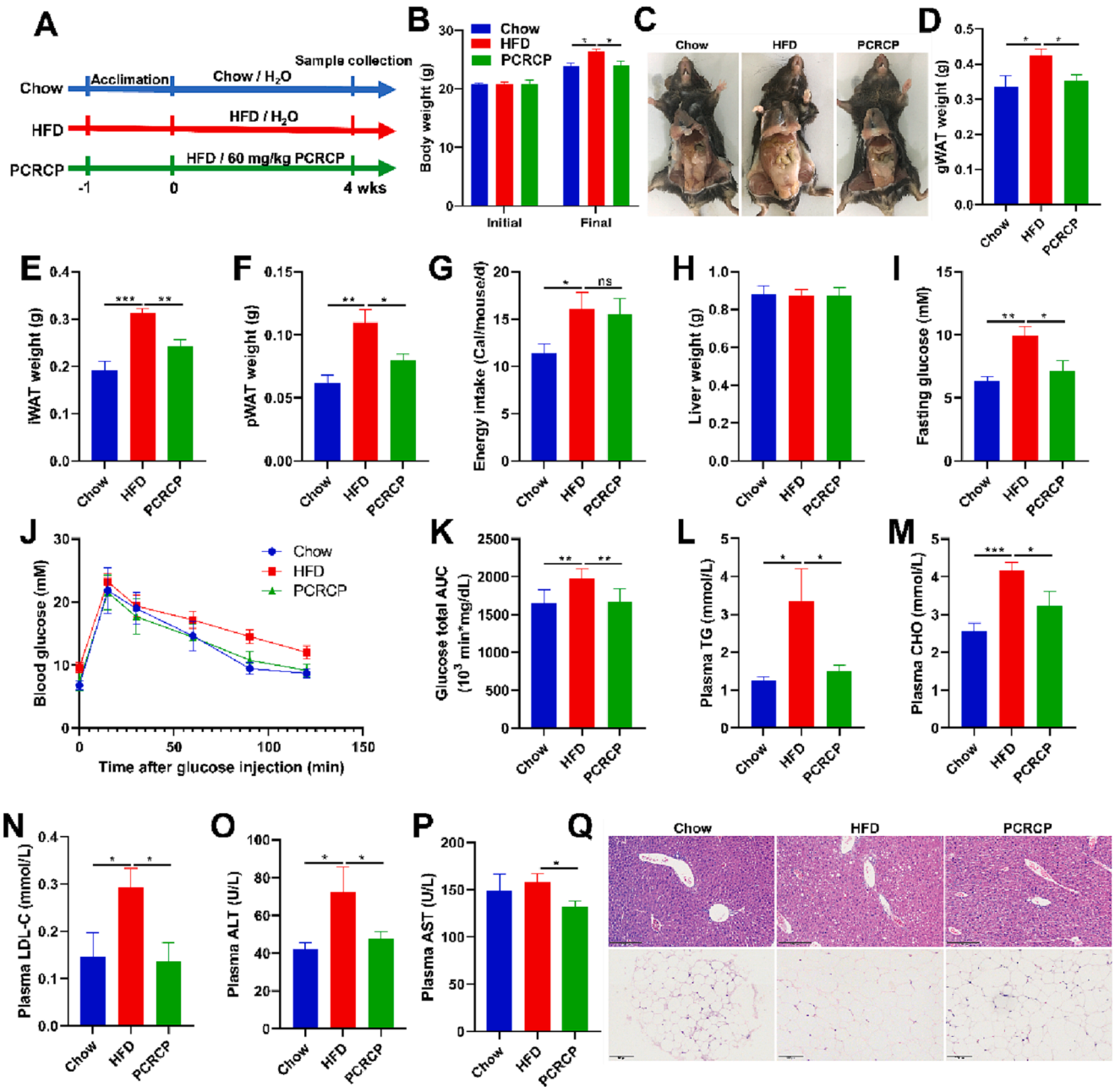

Fig. 2. PCRCP treatment prevents obesity and metabolic abnormalities in mice fed with HFD. (A) Schematic diagram of experiment. Animals were administered with Chow or HFD feeding, and orally given H_2O or 60 mg/kg/d PCRCP for four weeks. (B) The initial and final body weights of mice. (C) Representative photographs of gonadal adipose tissue of mice. (D-F) Visceral fat pad weights (gonadal, inguinal and perirenal white adipose tissues). (G) Average daily energy intake of mice. (H) Liver weight. (I) The level of fasting glucose. (J, K) Glucose tolerance and the area under curve. (L-P) The plasma levels of TG, CHO, LDL-C, ALT and AST of mice. (Q) Representative images of H&E staining for liver (scale bars, 200 μm) and gWAT (scale bars, 100 μm). Data are represented as the mean ± s.e.m. ($n = 5$–7). Statistical analysis was conducted by using one-way ANOVA followed by multiple comparisons, and *ns* means no statistical significance.

carbohydrate transport and metabolism, as well as insulin resistance (Fig. 3D-G). Notably, administration with PCRCP significantly regulated the mRNA expression of several lipidosis genes, including fatty acid-binding protein 5 (Fabp5), niemann-pick type C1 (Npc1) and encoding alkaline ceramidase 2 (Acer2), as well as stimulation on stearoyl-CoA desaturase (SCD2) and peroxisome proliferator-activated receptor-α (Ppargc1α) (Fig. 3H). Gene set enrichment analysis (GSEA) further confirmed significant enrichment of PCRCP-regulated genes that are directly involved in the modulation of oxidative phosphorylation and biosynthesis of unsaturated fatty acids (Fig. 3I). In short, these results indicate that the prevention of PCRCP against MetS induced by HFD may be related to the regulation of adipocyte lipogenesis and lipolysis in mice.

3.3.3. *PCRCP supplementation enhances gut barrier function and regulates gut microbiota composition alterations in HFD-fed mice*

A long-term HFD can cause gut dysbiosis such as leaky gut and dysregulated microbiota, leading to the development of MetS [7]. As intestinal flora can transform indigestible polysaccharides into beneficial metabolites such as SCFAs, thereby improving the intestinal microenvironment [11], we reasoned that the potential preventive effect of PCRCP for obesity may be dependent on the gut microbiota. Therefore, we first observed the effects of PCRCP on the gut integrity of mice. HFD feeding caused irregular ileal structures, eroded mucosa and

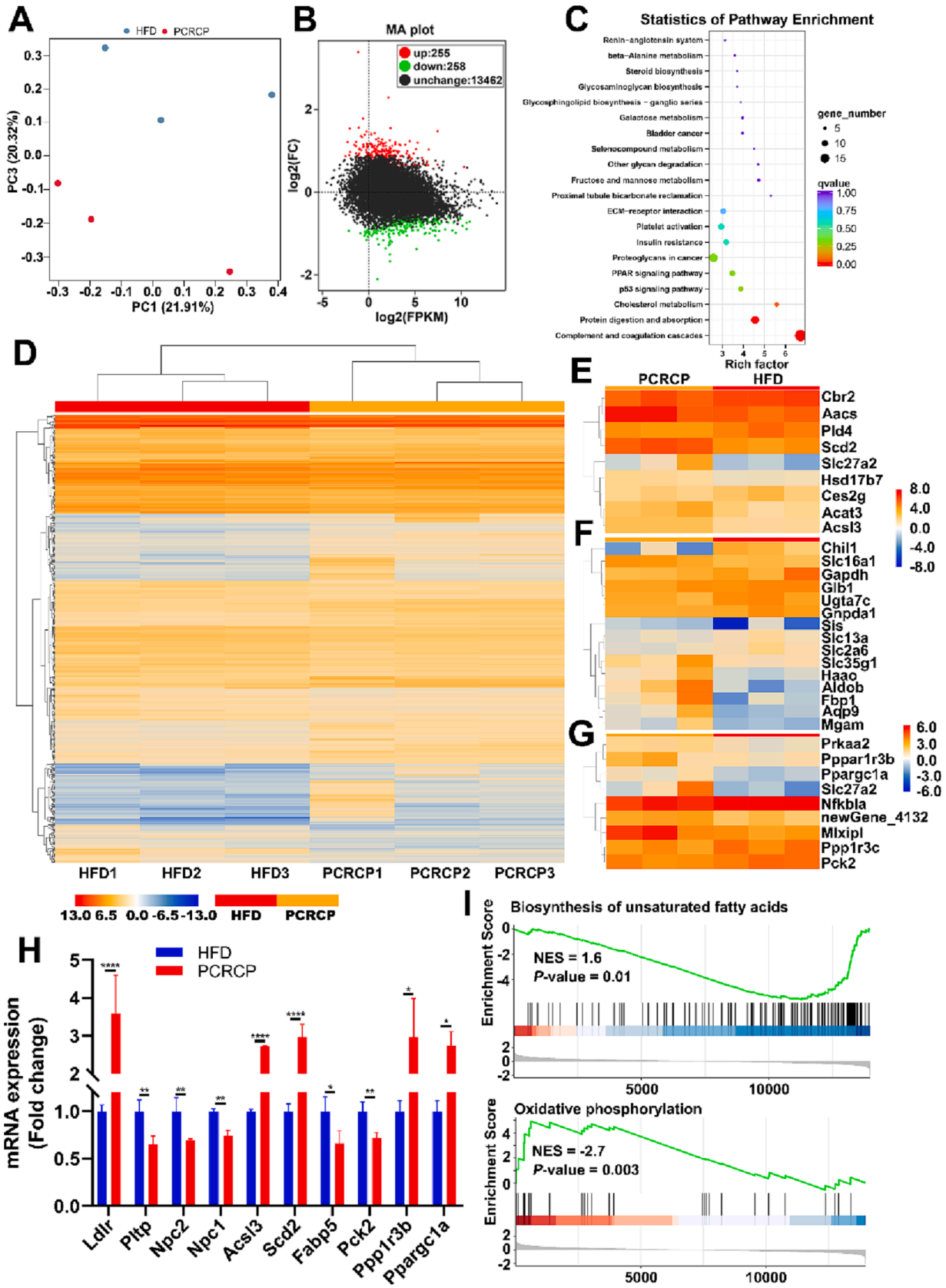

Fig. 3. PCRCP regulates molecular signaling pathways involved in obesity. The gene expression profiles of adipose tissue were performed by RNA_seq. (A) Principal component analysis (PCA). (B) M−versus−A plot analysis of expressed genes. (C) Pathway enrichments of differentially expressed genes were analyzed based on KEGG term. (D) Heatmap exhibiting differentially expressed genes. (E-G) Heatmap of differentially expressed genes of (E) lipid transport and metabolism, (F) carbohydrate transport and metabolism, and (G) insulin resistance based on enriched COG terms and GSEA. (H) The expressions of target genes from RNA-Seq analysis. (I) Geneset enrichment analysis.

extensive inflammatory cell infiltration, and a decrease in the number of mucus-secreting goblet cells in mice. These observations were in agreement with previous reports [5]. In contrast, treatment with PCRCP effectively preserved the length of intestinal villi and the integrity of mucosa, and decreased the infiltration of inflammatory cells (Fig. 4A). These data indicate that PCRCP could effectively alleviate HFD-induced ileitis symptoms.

Next, we examined the intestinal microbiota composition by 16S rRNA gene amplicon sequencing based on the PacBio platform. After elimination of the unqualified sequences, a total of 83,243 high-quality sequences and a total of 2127 OTUs were acquired from 15 fecal samples based on 97% of sequence similarity criterion (Table S6 and Fig. S2A).

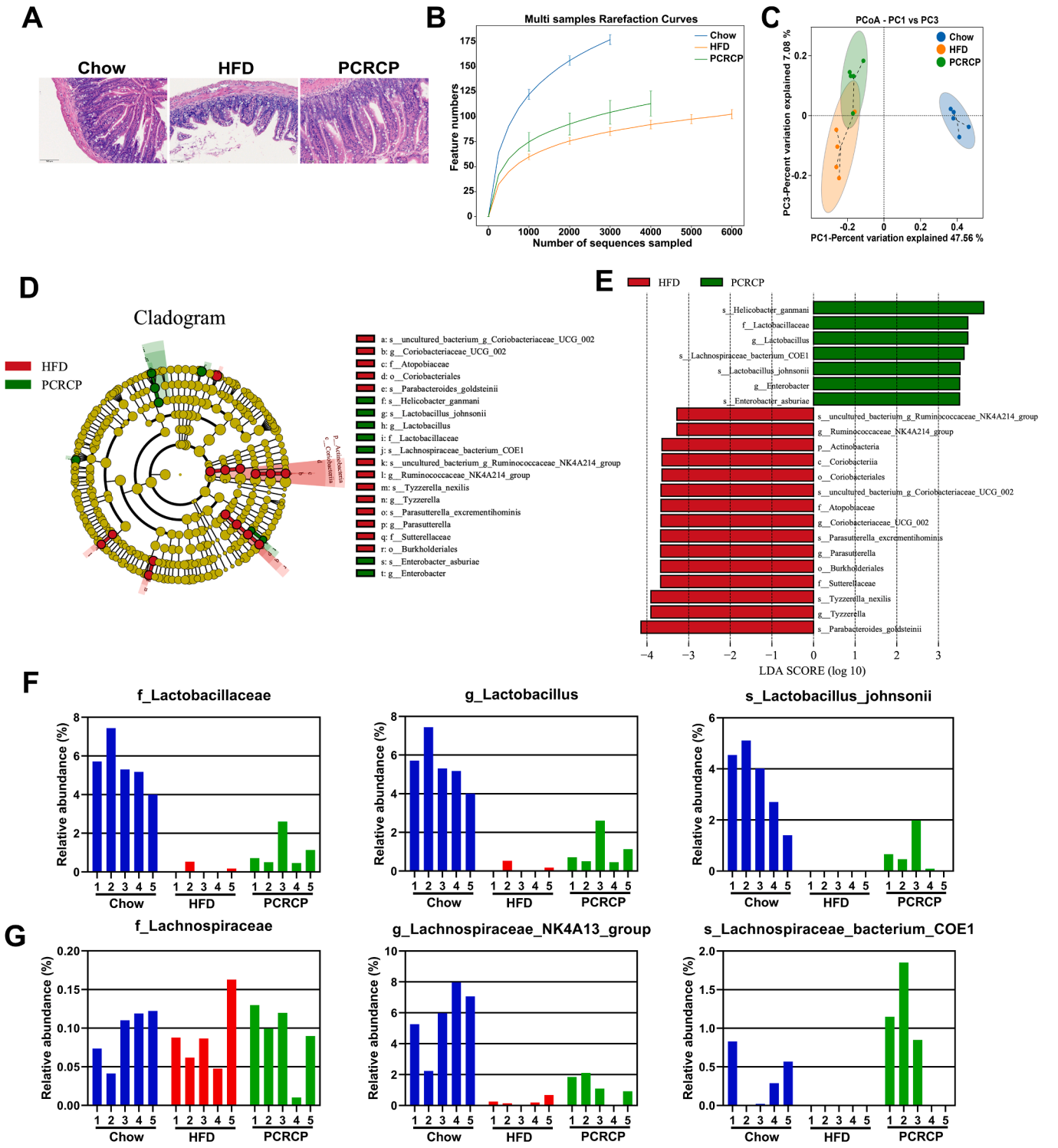

Fig. 4. PCRCP modulates the composition of gut microbiota induced by HFD in mice. (A) Representative pictures of H&E-staining for intestine (scale bars, 100 μm). (B) The multi samples rarefaction curves presented the α-diversity of gut microbiota. (C) The Weighted UniFrac PCoA analysis. (D) Analysis of differences in the microbial taxa exhibited by LEfSe and (E) its linear discriminant analysis (LDA) between HFD-fed mice and PCRCP-treated mice. (F, G) The relative abundance of (F) *Lactobacillaceae, Lactobacillus* and *Lactobacillus_johnsonii*, and (G) *Lachnospiraceae*, *Lachnospiraceae_NK4A13_group* and *Lachnospiraceae_bacterium_COE1* at the family-genus-species levels.

An increase in the number of OTUs and the α-diversity of the gut microbiome were observed in PCRCP-treated mice compare to HFD-fed mice (Fig. 4B and S2B-C). Additionally, relative to HFD-fed mice, the structure of the microbiota in PCRCP-treated mice was more closely clustered to Chow-fed mice (Fig. 4C), revealed that PCRCP effectively maintained or rebalanced HFD-induced gut microbiota dysbiosis to a healthy status.

We then further analyzed the degree of similarity of bacteria classification at different levels. An obvious decrease in the relative abundance of *Firmicutes,* a common signature of gut microbiota dysbiosis, was observed in HFD-induced mice relative to Chow-fed mice. In contrast, the relative abundance of *Firmicutes* was dramatically recovered by PCRCP supplementation (Fig. S2D). At the genus level, compared with HFD-fed mice, supplementation with PCRCP significantly changed the relative abundance of the six genera. Notably, treatment with PCRCP conspicuously increased the relative abundance of obesity-suppressing bacteria *Lactobacillus* and *Lachnospiraceae_NK4A136_group* [33], while simultaneously decreased the abundance of dyslipidemia-exacerbating bacteria *Coriobacteriaceae_UCG_002* in HFD-fed mice [16] (Fig. S2E). Among these bacterial genera, *Lachnospiraceae_NK4A136_group* and *Lactobacillus,* function as SCFA-producing bacteria in intestinal tract. For instance, the *Lachnospiraceae_NK4A136_group,* typical kind of butyrate-producing bacteria, has been recently found to be positively correlated with the gut barrier integrity and fecal butyrate concentration, and negatively related with the plasma LPS level [15].

More significantly, *Lactobacillus spp* such as L. casei strain Shirota, L. gasseri, L. rhamnosus and L. plantarum, could produce *L*-lactate and regulate enterocyte lipid metabolism, glucose uptake, intestinal inflammatory response and barrier function [4,22]. Therefore, *Lactobacillus* exerts considerable anti-obesity effects most probably by improving glucose and lipid metabolism and insulin resistance. *Lactobacillus* strains have been regarded as one of the most effective probiotics for the prevention and treatment of MetS in both rodents and humans [20,41]. Similarly, we also identified the relative abundance of the top 30 bacterial genera and its correlations with metabolic phenotypes in mice treated with PCRCP. The relative abundances of *Lachnospiraceae_NK4A136_group* and *Lactobacillus* were negatively correlated with the body weight, and the plasma levels of TC, FG and TG (Fig. S3). Notably, *Lachnospiraceae_NK4A136_group* and *Lactobacillus* act as broad enterotypes of gut bacteria, have been found to play an important role in the regulation of key metabolic functions [30]. These alterations in the PCRCP-stimulated bacteria further highlight the potential benefits of PCRCP on the gut barrier function by the elevation of probiotics levels.

Because the gut microbiota composition at the phylum and genus levels could be changed by PCRCP treatment, we were keen to find out the pivotal phylotypes of gut microbiota corresponding to PCRCP. Thus, we performed LEfSe analysis to identify the specific microbes that are responsible for the regulation of the obesity in mice. We observed that the relative abundances of several species dramatically altered upon the administration of HFD or PCRCP. Notably, PCRCP administration significantly increased the levels of *Lactobacillus_johnsonii, Lachnospiraceae_ bacterium_COE1, Helicobacter_ganmani*, and *Enterobacter_asburiae*, and decreased the levels of *Tyzzerella_nexilis* and *Parasutterella_excrementihominis* in HFD-fed mice (Fig. 4D-E).

Notably, *Lactobacillus johnsonii* was the only clade that was considerably enriched at the family-genus-species levels in the microbiota of mice fed with HFD (Fig. 4F-G). *Lactobacillus johnsonii* was first classified with *Lactobacillus acidophilus* [42], and functions as known commensal bacteria with anti-obesogenic properties in both animals and human beings [37,38]. Various *Lactobacillus johnsonii* strains exhibit probiotic properties, including the suppression of the growth of pathogenic bacteria in the intestinal tract, reduction of glucose and lipid levels, and promotion of bacterial-intestinal epithelial cells adhesion. For example, *Lactobacillus johnsonii N6.2* exhibited the inactivation of the inflammasome-mediated inflammation in ileum tissue and low levels of obesity and MetS in HFD-fed rats [26]. *Lactobacillus acidophilus NS1* [18] *and Lactobacillus amylovorus KU4* [17] have also been shown to induce BAT activity or browning of WAT, decrease lipogenesis and lipid deposition, and ameliorate insulin resistance in mice fed with HFD. More importantly, our present observation that *Lactobacillus johnsonii* may be responsible for the efficacy of polysaccharides, was strongly supported by literature report that the *Lactobacillus johnsonii* could be enriched by the polysaccharides from Lyophyllum decastes, and supplementation of *Lactobacillus johnsonii* effectively reduced the obesity and hyperlipidemia in a mouse model of obesity [32]. Taken together, the anti-obesity effects and maintenance of gut integrity of PCRCP may be attributed to the alterations of specific bacteria in the intestinal microbiota in HFD-treated mice. In particular, PCRCP-enriched *Lactobacillus johnsonii* may help to effectively relieve the gut inflammation and obesity induced by HFD. However, more work will be needed to clarify the detailed mechanism of action.

3.3.4. Gut microbiota plays essential role in the anti-MetS effects of PCRCP

As above-mentioned results indicated that the anti-MetS effects of PCRCP are likely to be regulated by the specific bacteria *Lactobacillus johnsonii*, we depleted gut microbiota with a cocktail of antibiotics (ABX, containing ampicillin and neomycin) to assess whether gut microbiota mediates a beneficial effect of PCRCP during the inhibition of obesity. HFD-fed mice were pretreated with ABX for one week (Fig. 5A). This pretreatment can suppress more than 90% of gut bacteria [24]. As a consequence, we observed that compared with HFD-fed mice, depletion of the gut microbiome impaired the preventive efficacy of PCRCP and failed to reduce the body weight, adipose depositions (gWAT, iWAT and pWAT), dyslipidemia (CHO and TG) and liver function (ALT and AST) in mice fed by HFD (Fig. 5B, D and E-N), whereas without any effect on food consumption of mice (Fig. 5C). In other words, the metabolic protection of PCRCP were significantly impaired by the depletion of gut microbiota by antibiotics cocktail. These results strongly suggest that the intestinal microbiota is needed to maintain the effects of PCRCP against metabolic disorder in vivo. More work will be done to clarify this new hypothesis. For example, fecal microbial transplantation may be used to identify the roles of specific species, in particular *Lactobacillus johnsonii*, in the anti-obesity of PCRCP. Furthermore, the anti-obesity of *Lactobacillus johnsonii* alone or in combination with PCRCP should be also explored by using germ-free animals.

4. Conclusion

In conclusion, we have obtained a water-soluble arabinan-rich pectic PCRCP with a molecular weight of 122.0 kDa. PCRCP is mainly composed of galacturonic acid, arabinose and galactose, which are linked *via* glycosidic bonds of 1,4-linked Gal(p)-UA, 1,4-linked Ara(f) and 1,4-linked Gal(p). Administration with PCRCP could regulate signaling pathways involved in the suppression of fatty acid *de novo* synthesis and the activation of β-oxidation in adipose tissue, and effectively ameliorate obesity induced by HFD exposure. HFD-induced gut microbiota dysbiosis could be validly reconstructed by PCRCP treatment. Notably, PCRCP supplementation significantly reduced the relative abundances of obesity-promoting bacteria, and selectively stimulated the growth of specific bacteria, especially *Lactobacillus johnsonii*. More importantly, microbiota ablation with broad-spectrum antibiotics mitigated the anti-obesity effects of PCRCP, suggests that gut microbiota is in charge of the anti-obesity effects of PCRCP, and PCRCP might serve as a potential ideal prebiotic for the prevention of obesity. This finding provides a novel anti-obese candidate for the modulation of gut microbiota. More work will be done, for example, by using metabolomics and proteomics methods to explore the specific gut microbiota-dependent pathways and detailed mechanisms of action that are responsible for the regulatory effect of PCRCP on obesity. The outcomes will be reported in due course.

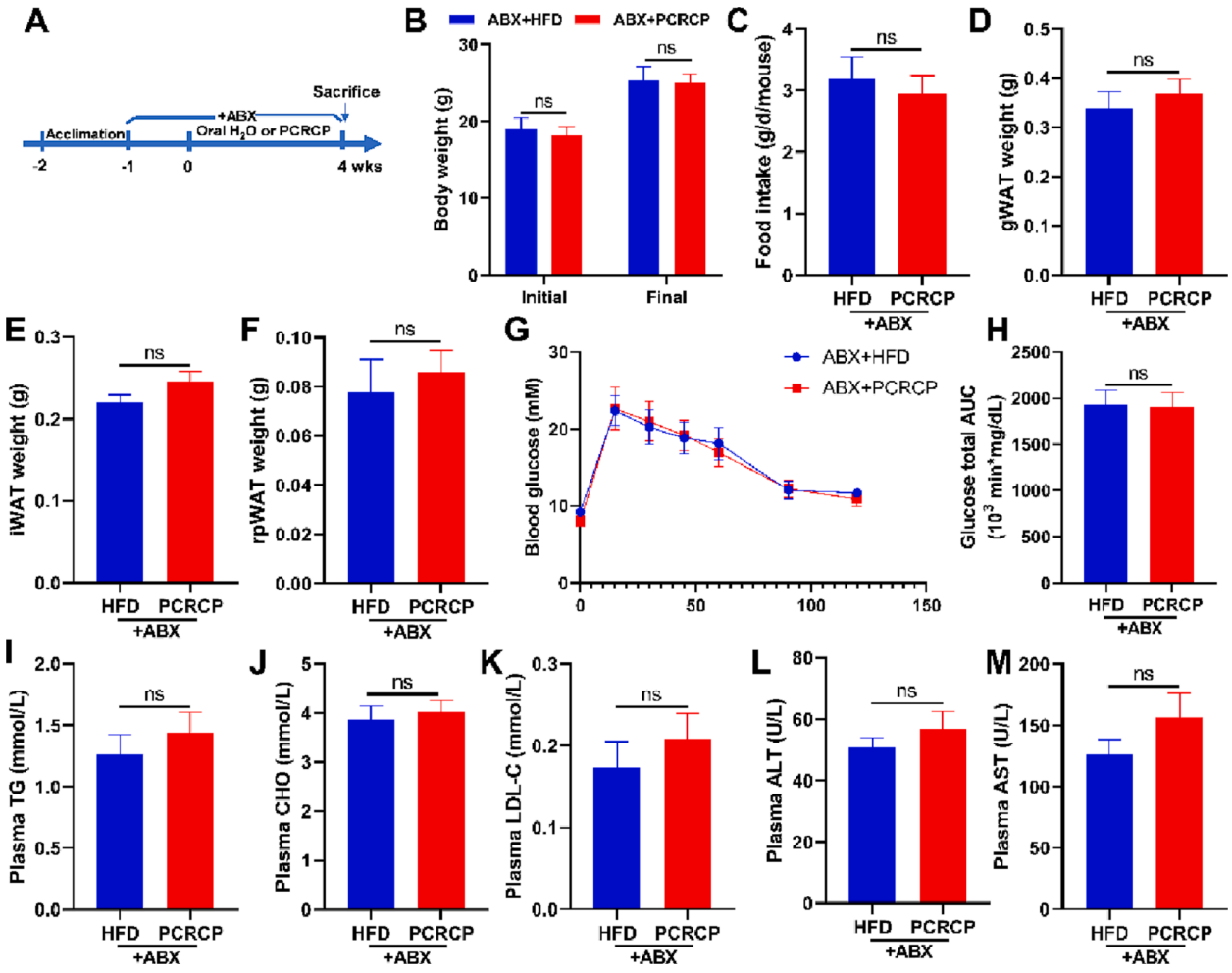

Fig. 5. Microbial depletion abolishes the anti-obesogenic effects of PCRCP in mice fed with HFD. (A) Diagram of antibiotics (vancomycin and neomycin) treatment of faecal bacteria. Animals were pretreated for one week with a cocktail of antibiotics added to the drinking water and provided orally with water or PCRCP for four weeks. (B) The initial and final body weight of mice. (C) The daily food intake of mice. (D-F) Visceral fat pad weight of gWAT, iWAT and pWAT. (G-H) Glucose tolerance and its area under curve. (I-M) The plasma levels of TG, CHO, LDL-C, ALT and AST. Data present the mean ± s.e.m. (n = 5–7). Statistical analysis was carried out by using Student's t-test, and ns means no statistical significance.

Declaration of Competing Interest

The authors declare that they have no known competing financial interests or personal relationships that could have appeared to influence the work reported in this paper.

Acknowledgements

This work was funded by the National Natural Science Foundation of China (Nos 82204035 and 81901678), the Department of Education of Guangdong Province (Nos 2019KZDZX2003, 2020KZDZX1203, 2021ZDZX4041 and 2022KQNCX094), Wuyi University (No 505170040415), Guangdong and Macao cooperation project from Department of Science and Technology of Guangdong Province and Jiangmen Science and Technology Bureau (2022A0505020026) and Fund of Zhejiang Provincial Department of Agriculture and Rural Affairs (2020XTTGZYC02).

Appendix A. Supplementary data

Supplementary data to this article can be found online at https://doi.org/10.1016/j.ultsonch.2023.106383.

References:

[1] A. Agus, K. Clément, H. Sokol, Gut microbiota-derived metabolites as central regulators in metabolic disorders, Gut 70 (6) (2021) 1174–1182, https://doi.org/10.1136/gutjnl-2020-323071.
[2] F.F. Anhê, R.T. Nachbar, T.V. Varin, J. Trottier, S. Dudonné, M.L. Barz, P. Feutry, G. Pilon, O. Barbier, Y. Desjardins, D. Roy, A. Marette, Treatment with camu camu (*Myrciaria dubia*) prevents obesity by altering the gut microbiota and increasing energy expenditure in diet-induced obese mice, Gut 68 (3) (2019) 453–464, https://doi.org/10.1136/gutjnl-2017-315565.
[3] L. Ang, H.W. Lee, A. Kim, M.S. Lee, Herbal medicine for the management of COVID-19 during the medical observation period: A review of guidelines, Integr Med Res. 9 (3) (2020), 100465, https://doi.org/10.1016/j.imr.2020.100465.
[4] J.R. Araujo, A. Tazi, O. Burlen-Defranoux, S. Vichier-Guerre, G. Nigro, H. Licandro, S. Demignot, P.J. Sansonetti, Fermentation products of commensal bacteria alter enterocyte lipid metabolism, Cell Host Microbe 27 (3) (2020) 358–375, https://doi.org/10.1016/j.chom.2020.01.028.
[5] K.E. Bouter, D.H. van Raalte, A.K. Groen, M. Nieuwdorp, Role of the gut microbiome in the pathogenesis of obesity and obesity-related metabolic dysfunction, Gastroenterology 152 (7) (2017) 1671–1678, https://doi.org/10.1053/j.gastro.2016.12.048.
[6] R.Z. Chen, C.G. Jin, Z.G. Tong, J. Lu, L. Tan, L. Tian, Q.Q. Chang, Optimization extraction, characterization and antioxidant activities of pectic polysaccharide from tangerine peels, Carbohydr. Polym. 136 (2016) 187–197, https://doi.org/10.1016/j.carbpol.2015.09.036.
[7] Y. Fan, O. Pedersen, Gut microbiota in human metabolic health and disease, Nat. Rev. Microbiol. 19 (1) (2021) 55–71, https://doi.org/10.1038/s41579-020-0433-9.
[8] F. Golbargi, S. Gharibzahedi, A. Zoghi, M. Mohammadi, R. Hashemifesharaki, Microwave-assisted extraction of arabinan-rich pectic polysaccharides from melon

peels: optimization, purification, bioactivity, and techno-functionality, Carbohydr. Polym. 256 (2021), 117522, https://doi.org/10.1016/j.carbpol.2020.117522.
[9] K. Hosomi, M. Saito, J. Park, H. Murakami, N. Shibata, A. Masahiro, T. Nagatake, K. Konishi, H. Ohno, K. Tanisawa, A. Mohsen, Y.A. Chen, H. Kawashima, Y. Natsume-Kitatani, Y. Oka, H. Shimizu, M. Furuta, Y. Tojima, K. Sawane, A. Saika, S. Kondo, Y. Yonejima, H. Takeyama, A. Matsutani, K. Mizuguchi, M. Miyachi, J. Kunisawa, Oral administration of Blautia wexlerae ameliorates obesity and type 2 diabetes via metabolic remodeling of the gut microbiota, Nat. Commun. 13 (1) (2022) 4477, https://doi.org/10.1038/s41467-022-32015-7.
[10] M. Kleinert, C. Clemmensen, S.M. Hofmann, M.C. Moore, S. Renner, S.C. Woods, P. Huypens, J. Beckers, M.H.D. Angelis, A. Schürmann, M. Bakhti, M. Klingenspor, M. Heiman, A.D. Cherrington, M. Ristow, H. Lickert, E. Wolf, P.J. Havel, T. D. Müller, M.H. Tschöp, Animal models of obesity and diabetes mellitus, Nat. Rev. Endocrinol. 14 (3) (2018) 140–162, https://doi.org/10.1038/nrendo.2017.161.
[11] H.B. Lee, Y.S. Kim, H.Y. Park, Pectic polysaccharides: targeting gut microbiota in obesity and intestinal health, Carbohydr. Polym. 287 (2022), 119363, https://doi.org/10.1016/j.carbpol.2022.119363.
[12] R.E. Ley, P.J. Turnbaugh, S. Klein, J.I. Gordon, Microbial ecology: human gut microbes associated with obesity, Nature 444 (7122) (2006) 1022–1023, https://doi.org/10.1038/4441022a.
[13] C. Liu, P. Du, Y.H. Guo, Y.F. Xie, H. Yu, W.R. Yao, Y.L. Cheng, H. Qian, Extraction, characterization of aloe polysaccharides and the in-depth analysis of its prebiotic effects on mice gut microbiota, Carbohydr. Polym. 261 (2021), 117874, https://doi.org/10.1016/j.carbpol.2021.117874.
[14] M.X. Luo, H.J. Luo, P.J. Hu, Y.T. Yang, B. Wu, G.D. Zheng, Evaluation of chemical components in Citri Reticulatae Pericarpium of different cultivars collected from different regions by GC-MS and HPLC, Food Sci. Nutr. 6 (2) (2018) 400–416, https://doi.org/10.1002/fsn3.569.
[15] L.Y. Ma, Y.H. Ni, Z. Wang, W.Q. Tu, L.Y. Ni, Z.G. Fen, A. Zhang, L.T. Hu, Y.F. Zhao, L.J. Zheng, Z.W. Fu, Spermidine improves gut barrier integrity and gut microbiota function in diet-induced obese mice, Gut Microbes 12 (1) (2020) 1–19, https://doi.org/10.1080/19490976.2020.1832857.
[16] H.N. Mu, Q. Zhou, R.Y. Yang, J. Zeng, X.H. Li, R.R. Zhang, W.Q. Tang, H.X. Li, S. M. Wang, T. Shen, X.Q. Huang, L. Dou, J. Dong, Naringin attenuates high fat diet induced non-alcoholic fatty liver disease and gut bacterial dysbiosis in mice, Front. Microbiol. 11 (2020), 585066, https://doi.org/10.3389/fmicb.2020.585066.
[17] S.S. Park, Y.J. Lee, H. Kang, G. Yang, E.J. Hong, J.Y. Lim, S.J. Oh, E. Kim, Lactobacillus amylovorus KU4 ameliorates diet-induced obesity in mice by promoting adipose browning through PPARgamma signaling, Sci. Rep. 9 (1) (2019) 20152, https://doi.org/10.1038/s41598-019-56817-w.
[18] S.S. Park, Y.J. Lee, S. Song, B. Kim, H. Kang, S. Oh, E. Kim, Lactobacillus acidophilus NS1 attenuates diet-induced obesity and fatty liver, J. Endocrinol. 237 (2) (2018) 87–100, https://doi.org/10.1530/JOE-17-0592.
[19] Z.S. Peng, S.R. Tian, H.L. Li, L.P. Zhu, Z.M. Zhao, G.D. Zheng, Q.Y. Wen, H.R. Tian, D.P. Yang, Extraction, characterization, and antioxidant properties of cell wall polysaccharides from the pericarp of Citrus Reticulata cv, Chachiensis. Food Hydrocolloid. 136 (2023), 108237, https://doi.org/10.1016/j.foodhyd.2022.108237.
[20] X. Qiu, Q. Wu, W. Li, K. Tang, J. Zhang, Effects of Lactobacillus supplementation on glycemic and lipid indices in overweight or obese adults: a systematic review and meta-analysis, Clin. Nutr. 41 (8) (2022) 1787–1797, https://doi.org/10.1016/j.clnu.2022.06.030.
[21] Q. Shang, H. Jiang, C. Cai, J. Hao, G. Li, G. Yu, Gut microbiota fermentation of marine polysaccharides and its effects on intestinal ecology: An overview, Carbohydr. Polym. 179 (2018) 173–185.
[22] B. Shirouchi, K. Nagao, M. Umegatani, A. Shiraishi, Y. Morita, S. Kai, T. Yanagita, A. Ogawa, Y. Kadooka, M. Sato, Probiotic Lactobacillus gasseri SBT2055 improves glucose tolerance and reduces body weight gain in rats by stimulating energy expenditure, Br. J. Nutr. 116 (3) (2016) 451–458, https://doi.org/10.1017/S0007114516002245.
[23] I.M. Sims, S.M. Carnachan, T.J. Bell, S. Hinkley, Methylation analysis of polysaccharides: technical advice, Carbohydr. Polym. 188 (2018) 1–7, https://doi.org/10.1016/j.carbpol.2017.12.075.
[24] V. Singh, B.S. Yeoh, B. Chassaing, X. Xiao, P. Saha, R. Aguilera Olvera, J. D. Lapek Jr., L. Zhang, W.B. Wang, S. Hao, M.D. Flythe, D.J. Gonzalez, P.D. Cani, J. R. Conejo-Garcia, N. Xiong, M.J. Kennett, B. Joe, A.D. Patterson, A.T. Gewirtz, M. Vijay-Kumar, Dysregulated microbial fermentation of soluble fiber induces cholestatic liver cancer, Cell 175 (3) (2018) 679–694, https://doi.org/10.1016/j.cell.2018.09.004.
[25] P. Sun, M. Wang, Z. Li, J. Wei, F. Liu, W. Zheng, X. Zhu, X. Chai, S. Zhao, Eucommiae cortex polysaccharides mitigate obesogenic diet-induced cognitive and social dysfunction via modulation of gut microbiota and tryptophan metabolism, Theranostics 12 (8) (2022) 3637–3655.
[26] L.D. Teixeira, L.M. Torrez, E. DeBose-Scarlett, E. Bahadiroglu, T.J. Garrett, C. L. Gardner, J.L. Meyer, G.L. Lorca, C.F. Gonzalez, Lactobacillus johnsonii N6.2 and blueberry phytophenols affect lipidome and gut microbiota composition of rats under high-fat diet, Front. Nutr. 8 (2021), 757256, https://doi.org/10.3389/fnut.2021.757256.
[27] C. Tian, H. Xu, J. Li, Z. Han, Characteristics and intestinal immunomodulating activities of water-soluble pectic polysaccharides from Chenpi with different storage periods, J. Sci. Food Agric. 98 (10) (2018) 3752–3757, https://doi.org/10.1002/jsfa.8888.
[29] I.S. Waddell, C. Orfila, Dietary fiber in the prevention of obesity and obesity-related chronic diseases: From epidemiological evidence to potential molecular mechanisms, Crit. Rev. Food Sci. Nutr. 1–16 (2022), https://doi.org/10.1080/10408398.2022.2061909.
[30] B.X. Wang, H.S. Yu, Y. He, L.K. Wen, J.D. Gu, X.Y. Wang, X.W. Miao, G.S. Qiu, H. R. Wang, Effect of soybean insoluble dietary fiber on prevention of obesity in high-fat diet fed mice via regulation of the gut microbiota, Food Funct. 12 (17) (2021) 7923–7937, https://doi.org/10.1039/d1fo00078k.
[31] H. Wang, G. Chen, X. Fu, R. Liu, Effects of aging on the phytochemical profile and antioxidative activity of Pericarpium Citri Reticulatae 'Chachiensis', RSC Adv. 6 (107) (2016) 105272–105281, https://doi.org/10.1039/C6RA22082G.
[32] T. Wang, J.J. Han, H.Q. Dai, J.Z. Sun, J. Ren, W.Z. Wang, S.S. Qiao, C. Liu, L. Sun, S.J. Liu, D.P. Li, S.L. Wei, H.W. Liu, Polysaccharides from Lyophyllum decastes reduce obesity by altering gut microbiota and increasing energy expenditure, Carbohydr. Polym. 295 (2022), 119862, https://doi.org/10.1016/j.carbpol.2022.119862.
[33] X.L. Wang, Z.M. Yang, X. Xu, H. Jiang, C. Cai, G.L. Yu, Odd-numbered agaro-oligosaccharides alleviate type 2 diabetes mellitus and related colonic microbiota dysbiosis in mice, Carbohydr. Polym. 240 (2020), 116261, https://doi.org/10.1016/j.carbpol.2020.116261.
[34] J.F. Wardman, R.K. Bains, P. Rahfeld, S.G. Withers, Carbohydrate-active enzymes (CAZymes) in the gut microbiome, Nat. Rev. Microbiol. 20 (9) (2022) 542–556, https://doi.org/10.1038/s41579-022-00712-1.
[35] J.X. Wu, X.T. Ye, S.H. Yang, H. Yu, L.Y. Zhong, Q.F. Gong, Systems pharmacology study of the anti-liver injury mechanism of Citri Reticulatae Pericarpium, Front Pharmaco. 12 (2021), 618846, https://doi.org/10.3389/fphar.2021.618846.
[36] T.R. Wu, C.S. Lin, C.J. Chang, T.L. Lin, J. Martel, Y.F. Ko, D.M. Ojcius, C.C. Lu, J. D. Young, H.C. Lai, Gut commensal Parabacteroides goldsteinii plays a predominant role in the anti-obesity effects of polysaccharides isolated from Hirsutella sinensis, Gut 68 (2) (2019) 248–262, https://doi.org/10.1136/gutjnl-2017-315458.
[37] J. Xin, D. Zeng, H.S. Wang, X.Q. Ni, D. Yi, K.C. Pan, B. Jing, Preventing non-alcoholic fatty liver disease through Lactobacillus johnsonii BS15 by attenuating inflammation and mitochondrial injury and improving gut environment in obese mice, Appl. Microbiol. Biotechnol. 98 (15) (2014) 6817–6829, https://doi.org/10.1007/s00253-014-5752-1.
[38] G. Yang, E. Hong, S. Oh, E. Kim, Non-viable Lactobacillus johnsonii JNU3402 protects against diet-induced obesity, Foods. 9 (10) (2020), https://doi.org/10.3390/foods9101494.
[39] Q. Yu, Y.X. Tao, Y.T. Huang, D. Zogona, T. Wu, R.T. Liu, Y. Pan, X. Xu, Aged Pericarpium Citri Reticulatae 'Chachi' attenuates oxidative damage induced by tert-butyl hydroperoxide (t-BHP) in HepG2 cells, Foods. 11 (3) (2022), https://doi.org/10.3390/foods11030273.
[40] S.L. Zeng, S.Z. Li, P.T. Xiao, Y.Y. Cai, C. Chu, B.Z. Chen, P. Li, J. Li, E.H. Liu, Citrus polymethoxyflavones attenuate metabolic syndrome by regulating gut microbiome and amino acid metabolism, Sci. Adv. 6 (1) (2020), x6208, https://doi.org/10.1126/sciadv.aax6208.
[41] Q. Zhang, X.Y. Fan, Y.J. Cao, T.T. Zheng, W.J. Cheng, L.J. Chen, X.C. Lv, L. Ni, P. F. Rao, P. Liang, The beneficial effects of Lactobacillus brevis FZU0713-fermented Laminaria japonica on lipid metabolism and intestinal microbiota in hyperlipidemic rats fed with a high-fat diet, Food Funct. 12 (16) (2021) 7145–7160, https://doi.org/10.1039/d1fo00218j.
[42] J.S. Zheng, S. Wittouck, E. Salvetti, C. Franz, H. Harris, P. Mattarelli, P.W. O'Toole, B. Pot, P. Vandamme, J. Walter, K. Watanabe, S. Wuyts, G.E. Felis, M.G.G. S. Lebeer, A taxonomic note on the genus Lactobacillus: Description of 23 novel genera, emended description of the genus Lactobacillus Beijerinck 1901, and union of Lactobacillaceae and Leuconostocaceae, Int. J. Syst. Evol. Microbiol. 70 (4) (2020) 2782–2858, https://doi.org/10.1099/ijsem.0.004107.

Further reading

[28] Z.J. Tan, C.Y. Wang, Y.J. Yi, H.Y. Wang, W.L. Zhou, S.Y. Tan, F.F. Li, Three phase partitioning for simultaneous purification of aloe polysaccharide and protein using a single-step extraction, Process Biochem. 50 (3) (2015) 482–486, https://doi.org/10.1016/j.procbio.2015.01.004.